Electronic Supplementary Material (ESI) for Nanoscale.
This journal is © The Royal Society of Chemistry 2020

Supporting information

Synthesis of Gadolinium/Iron-Bimetal-Phenolic Coordination Polymer Nanoparticles for Theranostic Applications

*Jing Qin, Guohai Liang, Youyou Feng, Bingxi Feng, Gen Wang, Na Wu, Yongxi Zhao, Jing Wei**

Experiment

1.1 Chemicals

Tannic acid (TA), $Gd(NO_3)_3 \cdot 6H_2O$, $FeSO_4 \cdot 7H_2O$ and polyvinylpyrrolidone (PVP, M_w=58000 g mol^{-1}) were purchased from Macklin Biochemical Co., Ltd. Calcein acetoxymethyl ester (calcein AM), propidium iodide (PI), 3-(4, 5-dimethylthiazol-2-yl)-2, 5-dipheny-ltetrazolium bromide (MTT) and Dulbecco's modified Eagle's medium (DMEM) were purchased from Sigma-Aldrich Co. (St Louis, USA). Ammonia solution (25 wt%), formaldehyde solution (37 wt%) and dimethyl sulfoxide (DMSO) were purchased from Tianjin Zhiyuan Chemical Co., Ltd. All reagents were used without further purification.

1.2 Synthesis of bimetal-phenolic coordination polymer nanoparticles

The bimetal-phenolic coordination polymer nanoparticles were synthesized via a metal-catechol coordination assembly process using TA as an organic ligand. Typically, PVP (0.3 g) was dissolved in the mixture of water (37 mL) and ethanol (8 mL) followed by addition of ammonia solution (0.5 mL, 25 wt %). Then, TA (0.2 g) and formaldehyde solution (0.38 mL, 37 wt %) were added to the above solution. After stirring for 12 hours, metal precursor solution (different molar ratio of $Gd(NO_3)_3 \cdot 6H_2O$ and $FeSO_4 \cdot 7H_2O$ dissolved in 2 mL of water) was added. After stirring for 12 hours, the solution was transferred to autoclave for hydrothermal treatment (100 ºC for 12 hours). Then, the obtained coordination polymers were dialyzed against deionized water for 48 h to remove the unreacted monomer and other small molecules (*e.g.*, NH_4OH). The solid products were collected via a freeze-dried process. The obtained samples were denoted Gd-Fe(*x*:*y*)-TA (*x*:*y* refers the molar ratio

of Gd and Fe in the precursors). In order to change the molar ratio of Gd/Fe in the coordination polymers, different amounts of Gd and Fe precursors were used during the synthesis process. The amount of metal precursors (*i.e.*, $Gd(NO_3)_3 \cdot 6H_2O$ and $FeSO_4 \cdot 7H_2O$) used for synthesis of Gd-Fe(*x*:*y*)-TA (*e.g.*, 8:2, 7:3, 6:4, 5:5) was listed in Table S1. Comparably, metal-phenolic coordination polymers with single metal source were also synthesized using a similar procedure. The obtained samples were denoted Gd-TA and Fe-TA.

1.3 Characterizations of metal-phenolic coordination polymers

Atomic force microscope (AFM) images were collected using ScanAsyst mode in air (Dimension Icon, Veeco Instruments/Bruker, Germany). Transmission electron microscopy (TEM) images were obtained using JEM-F200 operated at an accelerating voltage of 200 kV. The contents of metal species in the coordination polymers were determined by inductively coupled plasma mass spectrometry (ICP-MS) using NexION 350D. X-ray photoelectron spectroscopy (XPS) experiments were carried out on a Kratos AXIS Ultra DLD system with Al K_α radiation. Dynamic light scattering (DLS) and Zeta potential of the samples were measured with Zetasizer Nano ZS (Malvern Instruments Ltd, UK).

1.4 Cytotoxicity assay

The viability and proliferation of cells were evaluated by methyl thiazolyl tetrazolium (MTT) assay using Hela as a model cell. Typically, Hela cells with a density of 1.0×10^4 were seeded in a 96-well plate and further incubated in DMEM containing FBS (10%) at 37 °C for overnight. Subsequently, the culture medium was removed. The cells were incubated in culture medium containing Gd-Fe(7:3)-TA coordination polymers with different concentrations for 12 h and washed with medium twice. Then, 20 μL (5 mg mL^{-1}) of MTT solution was added to each well and the plate was further incubated for 4 h to deoxidize MTT. Then the medium was removed out and 150 μL of DMSO was added into each well. Absorbance was measured at 570 nm by enzyme-linked immunosorbent assay reader.

For photothermal cytotoxicity assay, the cells were irradiated with 808 nm laser (1.0 W cm^{-2}, 5 min) and further incubated for another 12 h. The cell viability was

evaluated with MTT assay.

The therapeutic effects of Gd-Fe(7:3)-TA on Hela cells were further evaluated by live/dead cell staining assays. Hela cells were seeded in 8-well plate at a density of 5.0×10^5 cells per dish for 24 h. Then, the cells were incubated with sample solution for 6 h. For PTT, the cells were irradiated with 808 nm laser at 1.0 W cm^{-2} for 5 min. After 12 h of incubation, the culture medium was discarded, and cells were washed three times with PBS. Then the cells were stained with calcein-AM (20 nM) and PI (4 μM) solution in PBS buffer solution for 20 min. Finally, the cells were washed three times with PBS and imaged by confocal laser scanning microscope (CLSM). Green fluorescence of calcein-AM was excited at 488 nm and detected with a 500-550 nm bandpass filter. Red fluorescence of PI was excited at 633 nm and detected with a 660-710 nm bandpass filter.

1.5 MRI performance

To investigate the MRI performance of Gd-Fe(7:3)-TA in vitro, Gd-Fe(7:3)-TA and Gd-DTPA solution with various concentrations (0.07-2.5 mM) was used for MRI test. T_1-weighted magnetic resonance images were acquired using a Siemens 1.0 T MRI scanner with the following imaging parameters: repetition time, 330 *ms*; echo time, 18.2 *ms*; field of view, 100×100 mm^2; and slice thickness, 3.0 mm.

1.6 In vivo MRI

The animal procedures followed the guidelines of the regional ethics committee for animal experiments established by South China Normal University Institutional Animal Care and Use. Female BALB/C mice (~20 g, purchased from Southern Medical University, Guangzhou) were maintained in a controlled environment with a 12 h/12 h light/dark cycle and provided with food supply and fresh water ad libitum. EMT-6 tumor models were established by subcutaneous injection of 1.5×10^7 EMT-6 cells into the backside of the mice. When the tumor volume reached 50~80 mm^3, the mice were used for in vivo MRI studies.

To investigate the MRI performance of Gd-Fe(7:3)-TA *in vivo*, one mouse selected at random was anaesthetized using 80 μL of chloral hydrate (10 wt%). 200 μL of Gd-Fe(7:3)-TA (400 μg mL^{-1}) solution was injected into the tumor via the tail vein. MRI

was performed at the desired time points after injection. T_1-weighted MRI was acquired using a Siemens 1.0 T MRI scanner with the following imaging parameters: repetition time, 330 *ms*; echo time, 18.2 *ms*; field of view, 100×100 mm^2; and slice thickness, 3.0 mm.

The relative signal enhancement (*RSE*) was calculated according to the following equation:

$$RSE = \frac{SI_{post} - SI_{pre}}{SI_{pre}} \times 100\%$$

SI_{pre} and SI_{post} are the signal intensities before and after injection, respectively.

1.7 Biological distribution and metabolism investigation

For the study of *in vivo* biological distribution and metabolism of Gd-Fe(7:3)-TA, the coordination polymer solution (4 mg kg^{-1} mouse) was intravenously injected into BALB/C mice. T_1-weighted MR images were collected at 0, 0.25, 0.5, 1, 2, 4, 6 and 12 h post-injection. Simultaneously, EMT-6 tumor bearing mice were intravenously injected with Gd-Fe(7:3)-TA solution (4 mg kg^{-1}). The mice were executed at 4, 24 and 72 h post-injection, respectively. Then, the heart, liver, spleen, lung, kidney and tumor tissues were collected, washed with PBS, weighed after drying, and homogenized in cold PBS (1:2, w/v). The content of Gd and Fe of each tissue was measured by ICP-MS analysis. The percent injected dose (%ID) and the percent ID per gram (%ID/g) values were calculated using the following equation

$$\%ID = \frac{dose\ in\ tissue\ sample}{injected\ dose} \times 100\%$$

$$\%ID/g = \frac{\%ID}{weight\ of\ tissue(g)} \times 100\%$$

To study the metabolic pathway of Gd-Fe(7:3)-TA, the BALB/C mice were injected with Gd-Fe(7:3)-TA solution through the tail vein. Then the mice were housed in special cages for the collection of urine and feces. The samples of urine and feces were completely digested with aqua regia. Gadolinium content in each sample

was determined by ICP-MS. The digested feces samples were imaged using 1.0 T MRI instrument.

1.8 In vitro photothermal evaluation of Gd-Fe(7:3)-TA

Gd-Fe(7:3)-TA solutions with different concentrations (0, 0.5, 0.75, 1.0 and 1.5 mg mL^{-1}) were placed in a centrifuge tube (1.0 mL) and irradiated by an 808 nm laser with different power densities (1.0, 1.5, 2.0 and 2.5 W cm^{-2}) for 10 min. The temperature changes were recorded using a digital thermometer and infrared thermal imaging camera (FLIR, USA).

To calculate the photothermal conversion efficiency (η), 1 mL of Gd-Fe(7:3)-TA solution (1 mg mL^{-1}) was added in a quartz cuvette and irradiated at power density of 1.0 W cm^{-2} for 10 min, then cooled naturally to room temperature. The photothermal conversion efficiency was calculated using the following equation[1, 2]:

$$\eta = \frac{hA\left(\Delta T_{max,mix} - \Delta T_{max,H_2O}\right)}{I\left(1 - 10^{-A_\lambda}\right)} \times 100\%$$

where h was the heat transfer coefficient. A was the surface area of the sample well. $\Delta T_{max,H_2O}$ was the temperature change of water at equilibrium temperature. $\Delta T_{max,mix}$ was the temperature change of Gd-Fe(7:3)-TA solution at the maximum equilibrium temperature. I was the laser power. A_λ was the absorption intensity of Gd-Fe(7:3)-TA (1.0 mg mL^{-1}) at 808 nm.

hA was determined by applying the linear time data from the cooling period.

$$t = -\frac{\sum_i m_i C_{p,i}}{hA} ln\frac{\Delta T}{\Delta T_{max}}$$

where m and C_p were the mass and heat capacity of solvent (water) or Gd-Fe(7:3)-TA nanoparticles. The mass of Gd-Fe(7:3)-TA (1.0×10^{-6} Kg) was much lower than that of solvent (1.0×10^{-3} Kg). Therefore, the m and C of Gd-Fe(7:3)-TA were negligible. m_{H_2O} was 1.0×10^{-3} Kg, C_{p,H_2O} was 4.2×10^{3} J kg^{-1} $℃^{-1}$. $\Delta T_{max,mix}$ and

$\Delta T_{max,H_2O}$ were 34.6 ℃ and 4.3 ℃ respectively. hA was 0.0125. Thus, the photothermal conversion efficiency (η) of Gd-Fe(7:3)-TA was 37 %.

1.9 *In vivo* photothermal therapeutic efficiency of Gd-Fe(7:3)-TA

EMT-6 tumor bearing mice were used for *in vivo* photothermal therapy (PTT). When the volume of tumor was reached to 50~80 mm^3, the mice were randomly divided into four groups (n=5) and treated with PBS only (control group), Gd-Fe(7:3)-TA only (NPs group), PBS and laser (laser group), Gd-Fe(7:3)-TA and NIR laser (PTT group). For PTT group, the mice were intravenously injected with Gd-Fe(7:3)-TA solution (4 mg kg^{-1}). The tumors of mice were irradiated with an 808 nm laser at 1.0 W cm^{-2} for 5 min at 4 h post-injection. Tumor size and body weight were measured every other day for 18 days. The tumor volume was calculated using the formula: tumor volume = (width^2 × length)/2. Relative tumor volume was calculated as V/V_0, where V_0 was the tumor volume when the treatment was initiated. On 18th day, all the mice were euthanized, and the tumor tissues were excised and weighed. Simultaneously, the main organs (heart, liver, spleen, lung, kidney and tumor) of mice were excised, fixed in 4% neutral buffered formalin and processed routinely into paraffin. The organs and tumors were sectioned to slices of 4 μm thickness for hematoxylin & eosin (H&E) and HIF-1α staining and observed by a digital microscope (Leica QWin).

1.10 *In vivo* toxicity of Gd-Fe-TA

The BALB/C mice were intravenously injected with Gd-Fe(7:3)-TA solution (4 mg kg^{-1}). Five mice were sacrificed after 1- and 3-day injection respectively. The mice blood was collected by retro-orbital bleeding for hematology analysis. Meanwhile, major organs including heart, liver, spleen, lung and kidney from the injected mice were harvested, then fixed in 4% neutral buffered formalin, processed into paraffin, and stained with hematoxylin and eosin (H&E).

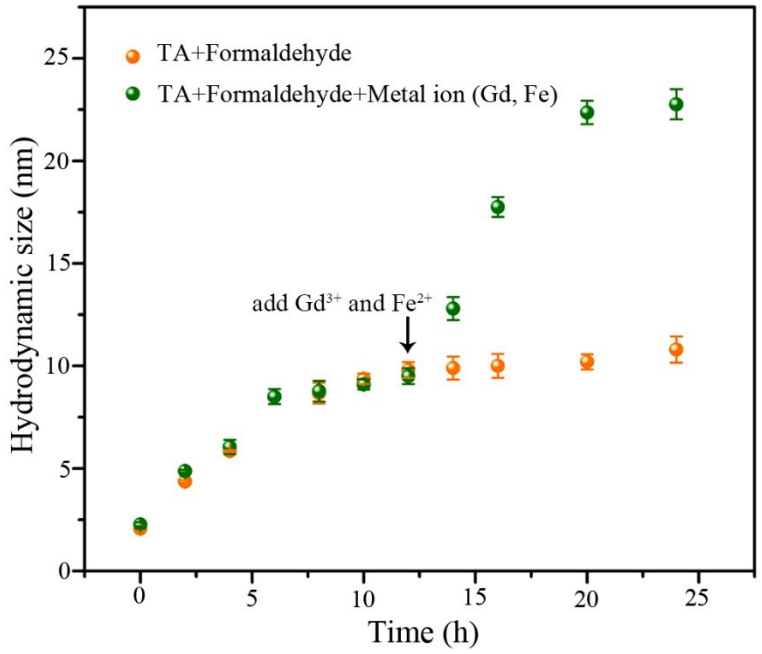

Figure S1 Hydrodynamic size of polymer oligomers during the polymerization process of tannic acid (TA) using formaldehyde and metal ions (Gd^{3+} and Fe^{2+}) as a crosslinker. For comparison, the hydrodynamic size of polymer nanoparticles crosslinked by formaldehyde only (without addition of metal species) was also investigated (yellow points).

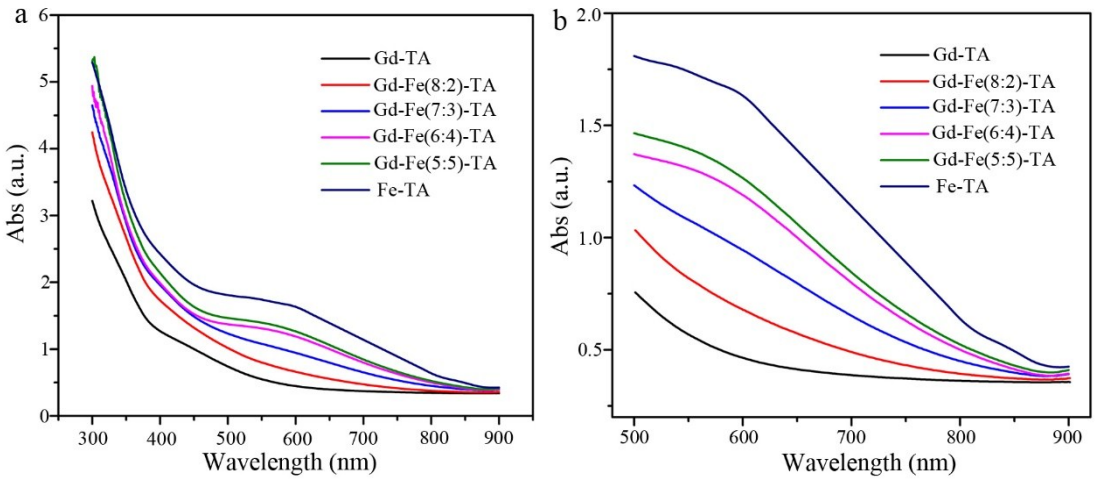

Figure S2 UV-vis spectra for different metal-phenolic coordination polymers (Gd-TA, Gd-Fe(8:2)-TA, Gd-Fe(7:3)-TA, Gd-Fe(6:4)-TA, Gd-Fe(5:5)-TA and Fe-TA). The concentration of the coordination polymers was 1.0 mg/mL. A broad peak at around 565 nm was ascribed to the ligand-to-metal charge transfer (LMCT) bands of TA/Fe(III), indicating the formation of metal-catechol coordination bond.

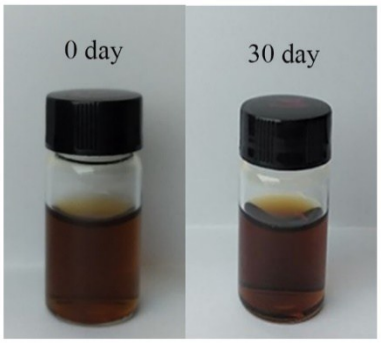

Figure S3 Photographs for Gd-Fe(7:3)-TA solution for different days (0 and 30 day).

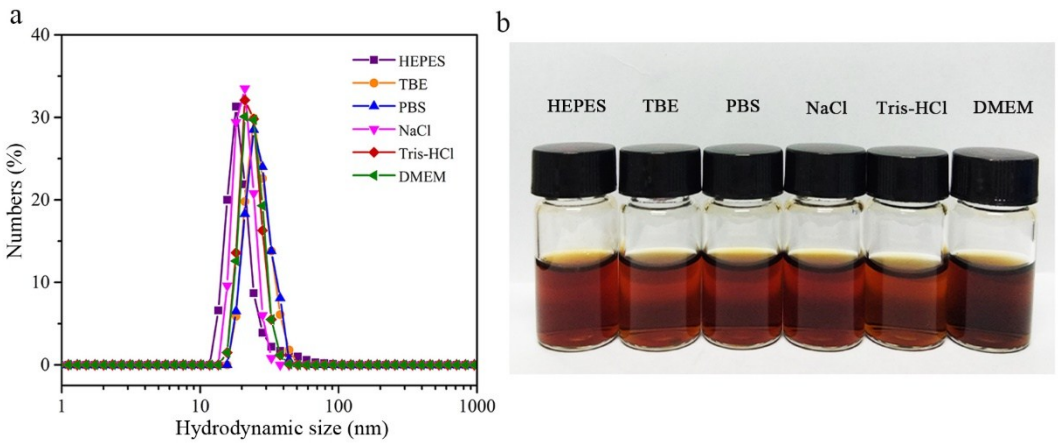

Figure S4 (a) DLS measurements of Gd-Fe(7:3)-TA in different kinds of solvents. (b) Photographs of Gd-Fe(7:3)-TA dispersed in different kinds of solvents: HEPES (pH=7.4, 0.01 M), TBE (pH=8.0, 1×), PBS (pH=7.3, 0.01M), NaCl (0.9 wt%), Tris-HCl (pH= 7.4) and DMEM supplemented with 10% FBS (v/v).

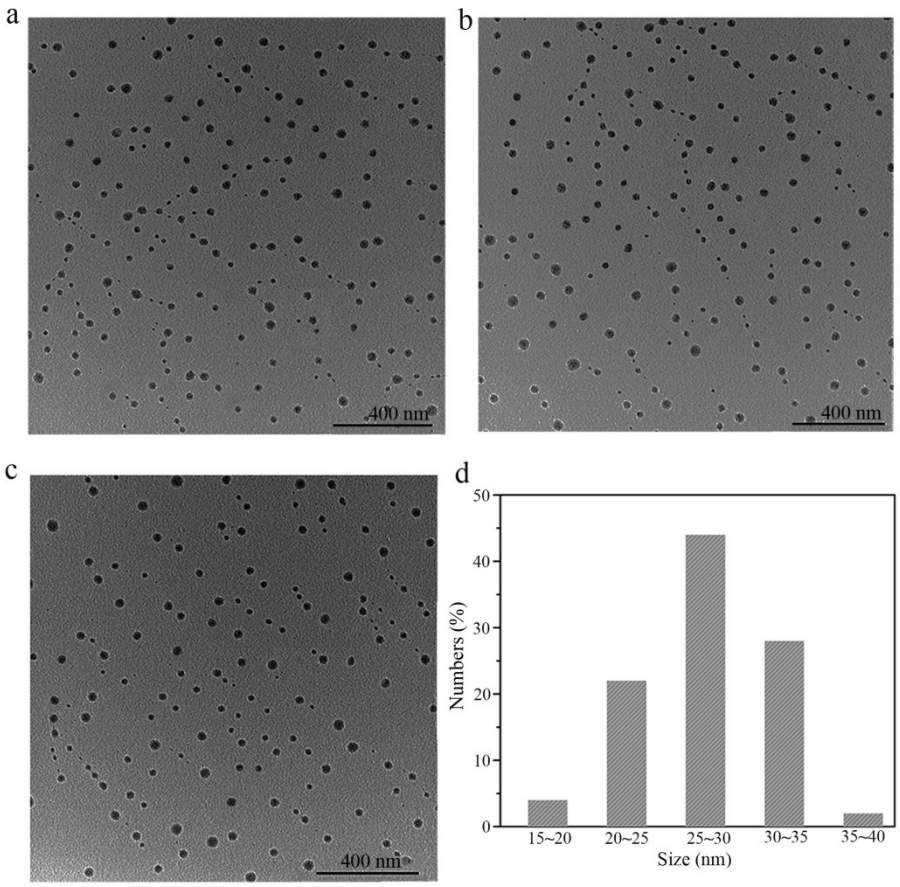

Figure S5 (a-c) TEM images and (d) corresponding curve-fitted histogram of sizes distribution for Gd-Fe(7:3)-TA coordination polymers.

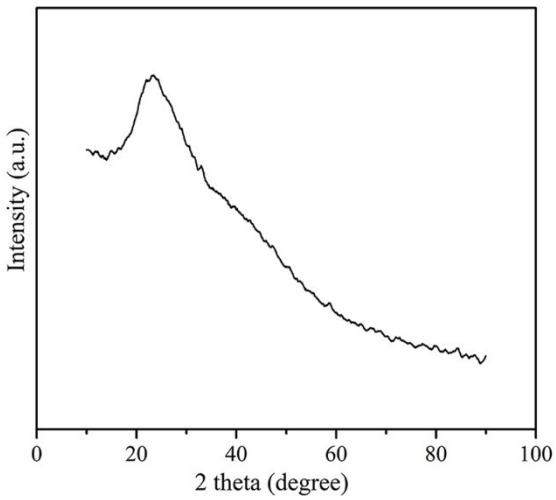

Figure S6 XRD patterns for Gd-Fe(7:3)-TA coordination polymers.

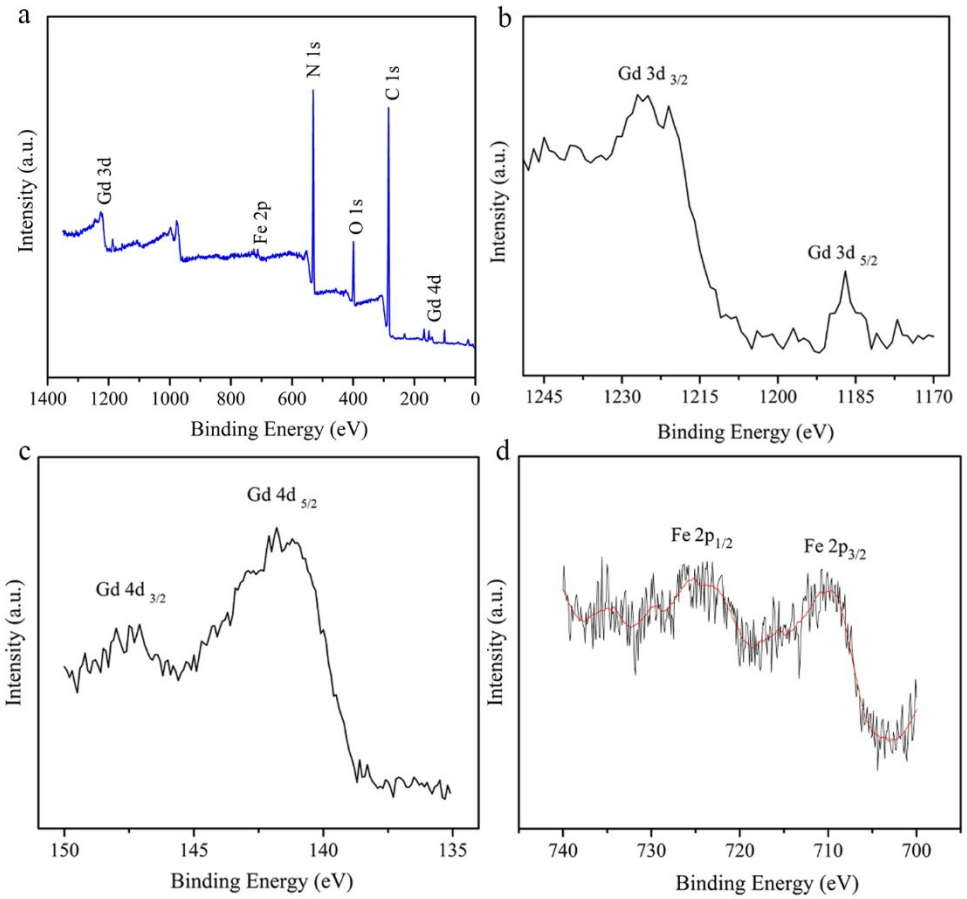

Figure S7 XPS for Gd-Fe(7:3)-TA coordination polymers, (a) survey spectra, (b) Gd 3d, (c) Gd 4d, and (d) Fe 2p spectra.

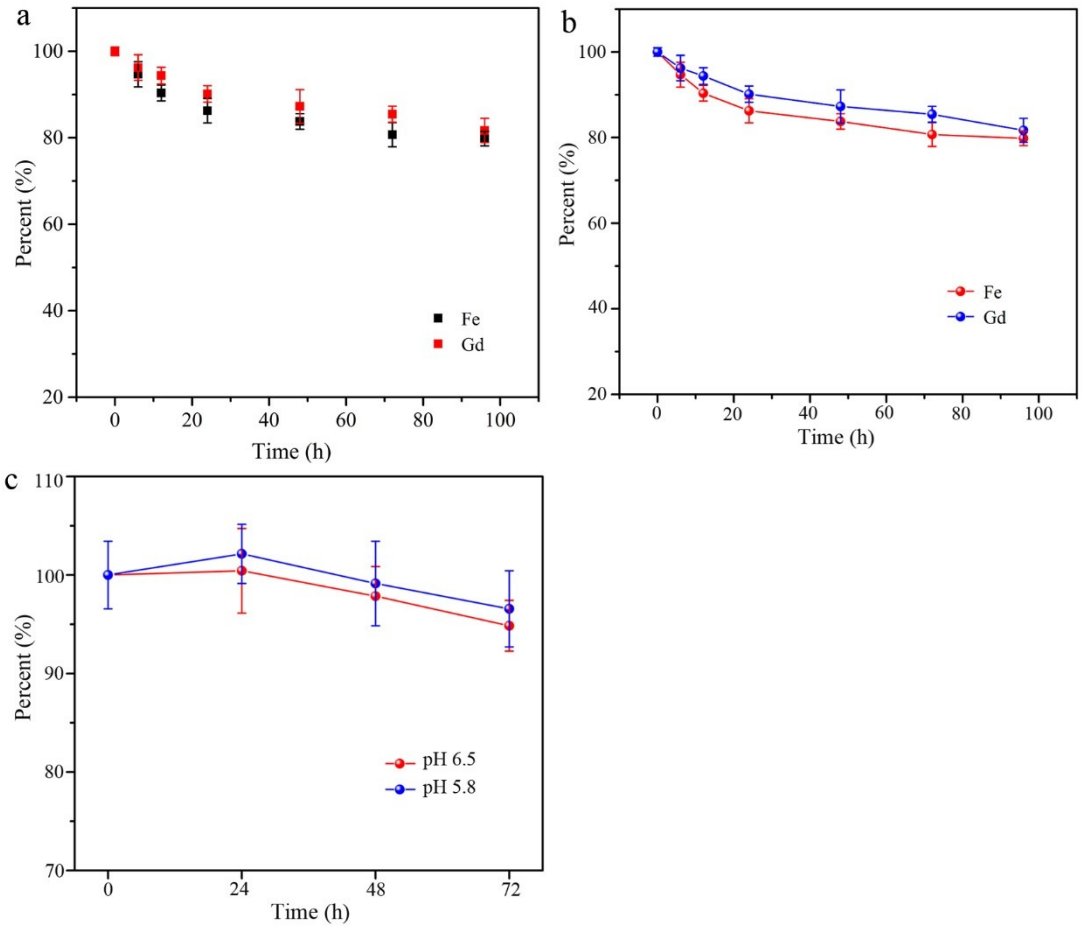

Figure S8 The contents of gadolinium and iron in Gd-Fe(7:3)-TA coordination polymers versus different dialysis times. (a) in water, (b) PBS solution, (c) Tris-HCl solution (pH 6.5 and 5.8). Gd-Fe(7:3)-TA coordination polymers also exhibited low leakage of Gd species in PBS and Tris-HCl (pH 6.5 and 5.8), indicating a high stability of the coordination polymers.

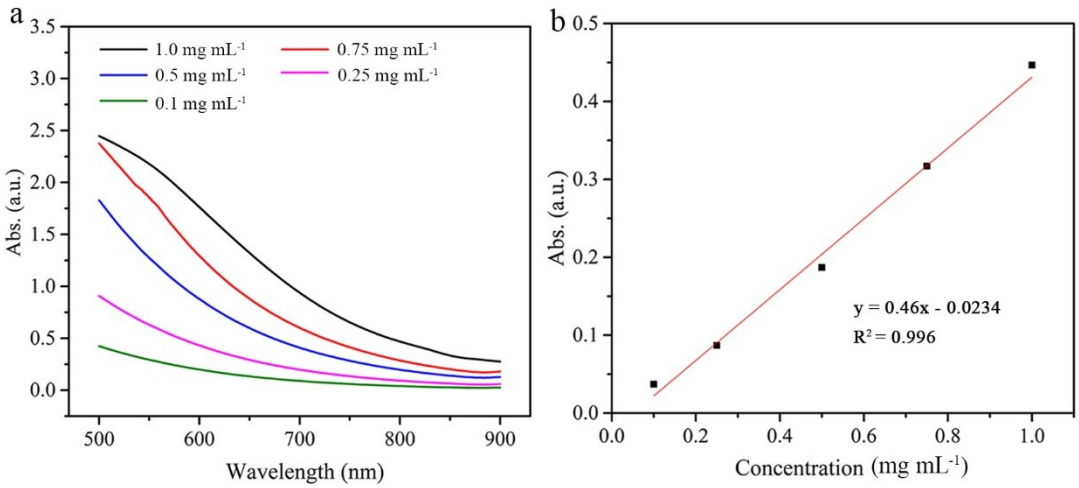

Figure S9 (a) UV-vis spectra of Gd-Fe(7:3)-TA solution at different concentrations (0.1-1.0 mg mL^{-1}). (b) The linear relationship for the optical absorbance at 808 nm as a function of the concentration of Gd-Fe(7:3)-TA solution.

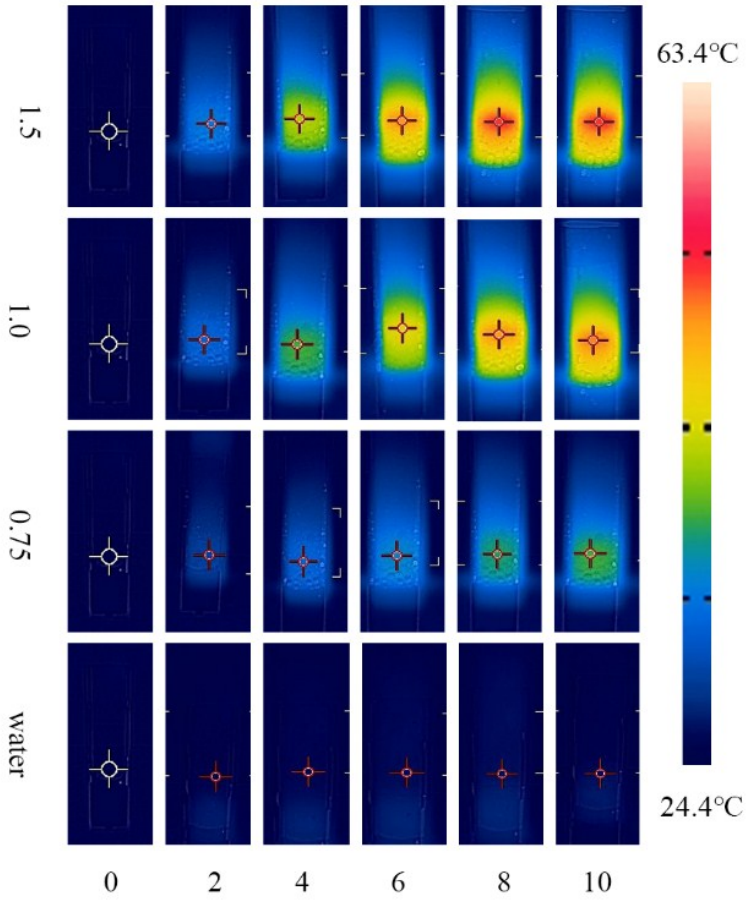

Figure S10 Infrared thermal images of Gd-Fe(7:3)-TA aqueous solutions with different concentrations (0.75, 1.0 and 1.5 mg mL^{-1}) irradiated with an 808 nm laser (1.0 W cm^{-2}) from 0 to 10 min.

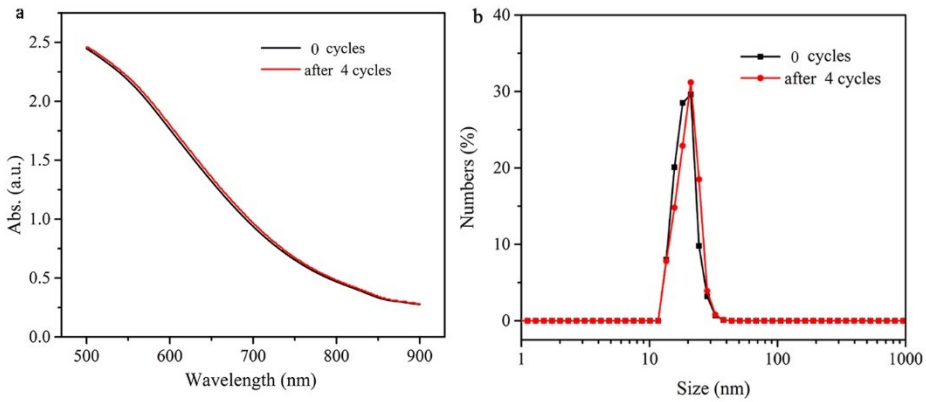

Figure S11 (a) The absorption spectra and (b) hydrodynamic size of Gd-Fe(7:3)-TA solution before and after four irradiation cycles.

.

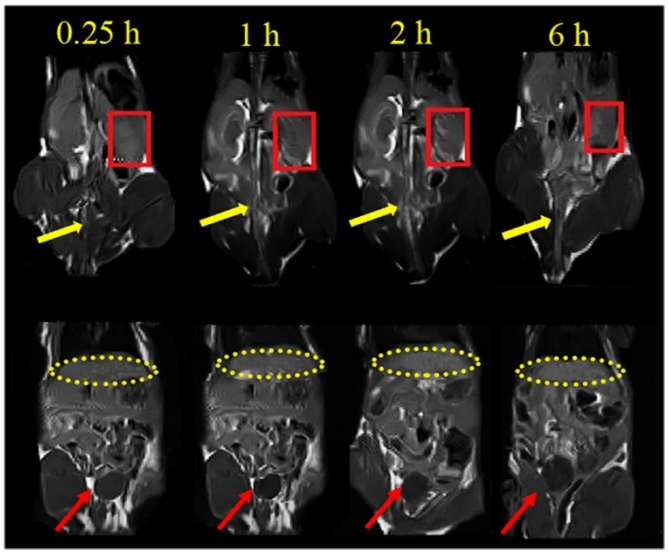

Figure S12 Representative MR images of a mouse at 0.25, 1, 2 and 6 h after intravenous injection. The yellow arrows, red arrows, red rectangles and yellow ellipses represented veins, bladder, kidney and liver respectively.

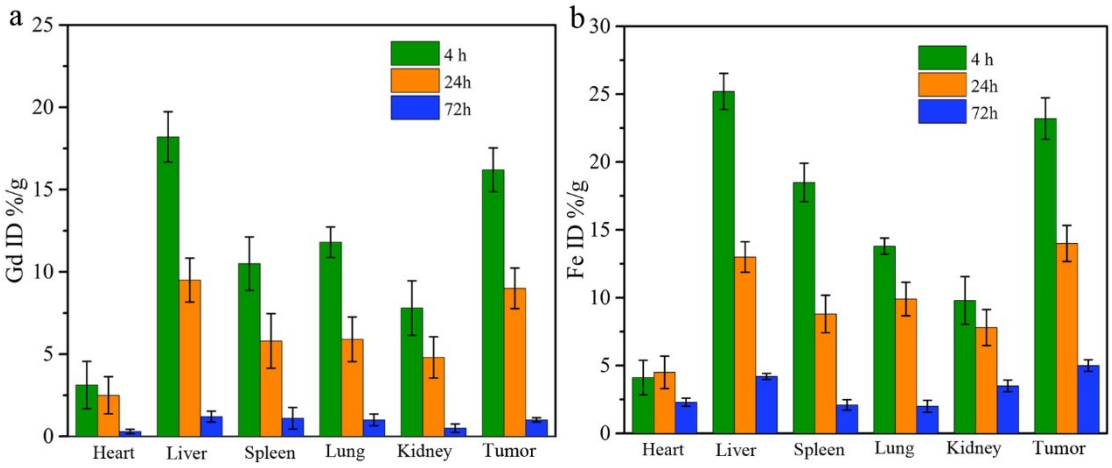

Figure S13 Biodistribution of (a) Gd and (b) Fe in major organs of mice at the 4, 24 and 72 h time point. Results are presented as mean ± S.D., n=5.

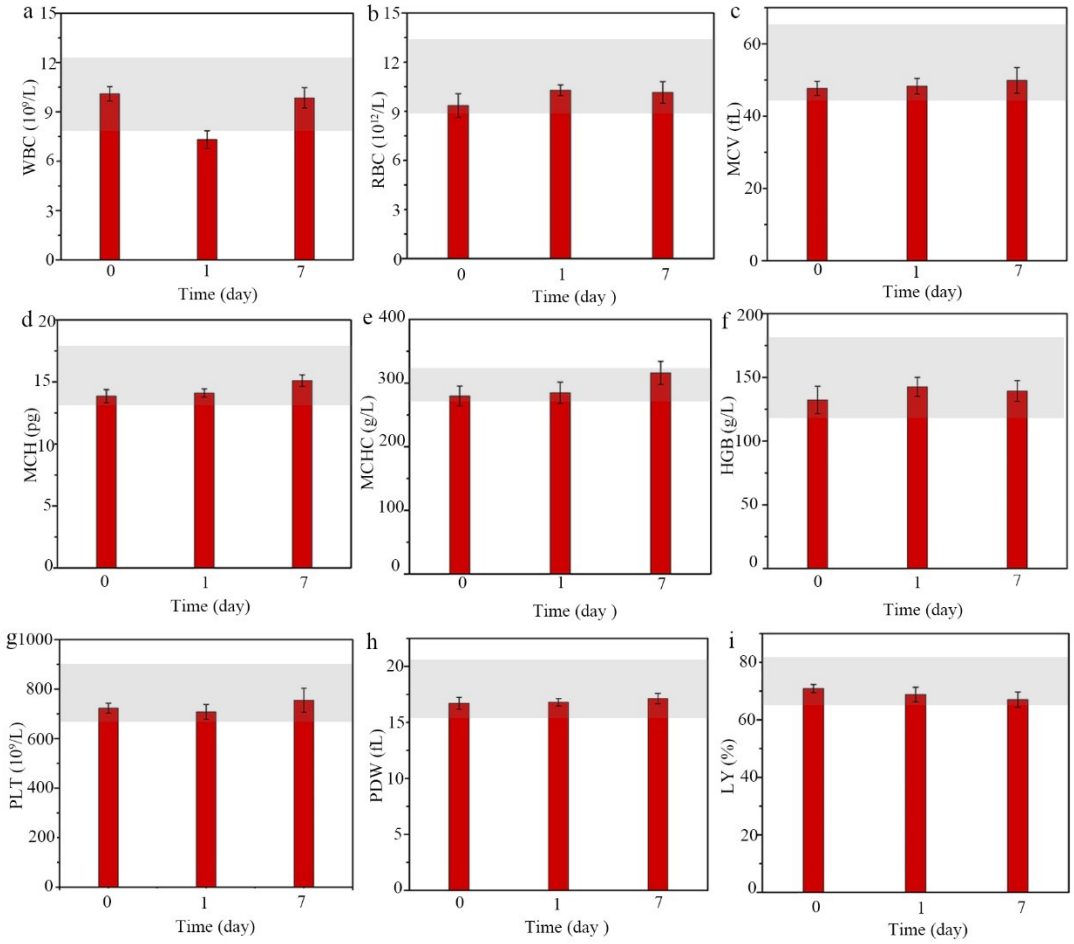

Figure S14 Hematology analysis of mice treated with Gd-Fe(7:3)-TA at different time points. (a) white blood cells (WBC), (b) red blood cell (RBC), (c) mean corpuscular volume (MCV), (d) mean corpuscular hemoglobin (MCH), (e) mean corpuscular hemoglobin concentration (MCHC), (f) hemoglobin (HGB), (g) platelets (PLT), (h) platelet distribution width (PDW), (i) lymphocyte count (LY).

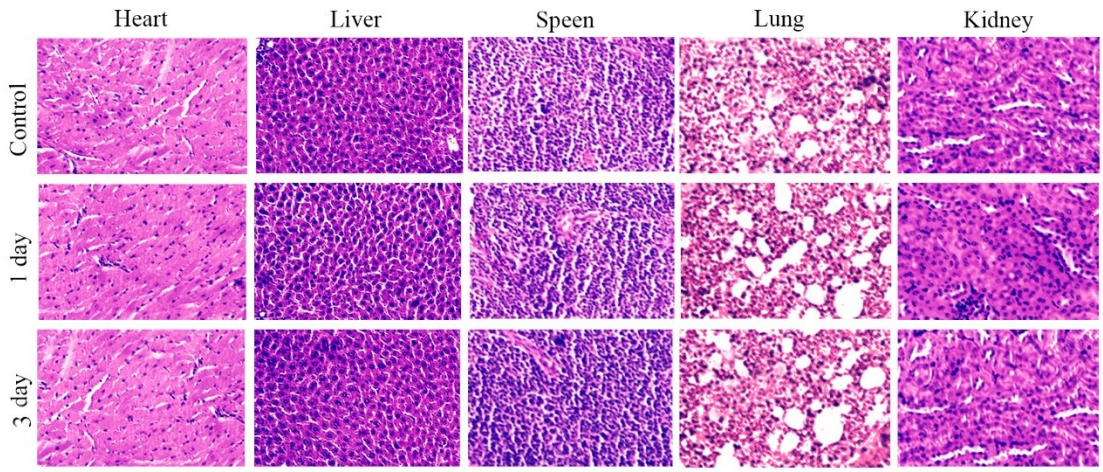

Figure S15 H&E staining of the different organs from mice after injection of Gd-Fe(7:3)-TA for 1 and 3 day. The injection of PBS in mice was used as a control group.

Table S1 The amount of the metal precursors and the compositions of the obtained metal-phenolic coordination polymers.

Sample	$Gd(NO_3)_3 \cdot 6H_2O$ (g)	$FeSO_4 \cdot 7H_2O$ (g)	Gd/Fe (at/at)[1]	Gd (S) (mg/g)[2]	Fe (S) (mg/g)[3]	Gd/Fe (S) (at/at)[4]
Gd-TA	0.1011	0	N.A.	74	0	N.A.
Gd-Fe(8:2)-TA	0.0808	0.0164	3.990	58	15	1.39
Gd-Fe(7:3)-TA	0.0696	0.0237	2.378	49	19	0.92
Gd-Fe(6:4)-TA	0.0602	0.0308	1.583	43	28	0.54
Gd-Fe(5:5)-TA	0.0477	0.0468	0.825	31	32	0.34
Fe-TA	0	0.1009	0	0	83	0

[1] Gd/Fe refers the molar ratio of Gd/Fe in the metal precursors.

[2] Gd (S) refers the mass content of Gd in the samples (coordination polymer).

[3] Fe (S) refers the mass content of Fe in the samples (coordination polymer).

[4] Gd/Fe (S) refers the molar ratio of Gd/Fe in the samples (coordination polymer).

Table S2 DLS and Zeta potential analysis of MPCSs with different molar ratios of Gd/Fe

Samples	Hydrodynamic size (nm)	Polydispersity index	ζ-potential (mV)
Gd-TA	25.4±1.58	0.232	-3.72±1.27
Gd-Fe(8:2)-TA	26.1±1.31	0.321	-4.35±1.38
Gd-Fe(7:3)-TA	23.2±1.21	0.368	-5.66±0.98
Gd-Fe(6:4)-TA	20.8±0.93	0.235	-5.28±0.81
Gd-Fe(5:5)-TA	27.6±1.38	0.473	-2.76±0.96
Fe-TA	21.9±0.86	0.424	-4.75±1.13

Table S3 DLS and Zeta potential analysis of Gd-Fe(7:3)-TA solutions with different dispersants: HEPES (pH=7.4, 0.01 M), TBE (pH=8.0, 1×), PBS (pH=7.3, 0.01M), NaCl (0.9 wt%), Tris-HCl (pH= 7.4) and DMEM supplemented with 10% FBS (v/v).

Dispersants	Hydrodynamic size (nm)	Polydispersity index	ζ-potential (mV)
HEPES	23.8±1.43	0.436	-4.81±1.45
TBE	24.7±1.42	0.422	-4.83±1.62
PBS	25.2±0.98	0.236	-5.64±1.32
NaCl	26.3±1.24	0.243	-4.89±0.97
Tris-HCl	26.1±1.09	0.353	-3.76±1.56
DMEM	25.4±0.97	0.451	-4.78±1.43

Table S4 Hydrodynamic size (nm), longitudinal relaxivity (r_1), transverse relaxivity (r_2) and photothermal conversion efficiency (η) for the metal-phenolic coordination polymers.

samples	Size (nm)	η *(%)*	H_0 *(T)*	r_1 ($mM^{-1}s^{-1}$)	r_2 ($mM^{-1}s^{-1}$)	r_2/r_1	reference
PNV@Fe-TA Hollow sphere	225-250	45.4	7	4.19	12.03	2.87	3
Fe(III)-TA	3000-4000	N.A.	9.4	2.04	12	5.9	4
Gd-TA	3000-4000	N.A	9.4	2.31	49	21.2	4
Fe-GA	5.3	N.A	1.5	1.5	2.9	1.9	5
Fe-EA	240	17.6	3.0	0.37	61.14	165	6
Fe/GA/PVP	6	67.4	3.0	2.16	3.09	1.43	7
Fe-GA-PEG	20	N.A.	1.0	3.5	0.97	0.28	8
Gd-Fe(7:3)-TA	23	37	1.0	9.3	11.8	1.26	**This work**

Reference

1 Y. Liu, K. Ai, J. Liu, M. Deng, Y. He, L. Lu, *Adv. Mater*., 2013, **25**, 1353-1359.

2 W. Ren, Y. Yan, L. Zeng, Z. Shi, A. Gong, P. Schaaf, D. Wang, J. Zhao, B. Zou, H. Yu, G. Chen, E. M. B. Brown, A. Wu, *Adv. Healthcare Mater*., 2015, **4**, 1526-1536.

3 T. Liu, M. Zhang, W. Liu, X. Zeng, X. Song, X. Yang, X. Zhang, J. Feng, *ACS Nano* 2018, **12**, 3917-3927.

4 J. Guo, Y. Ping, H. Ejima, K. Alt, M. Meissner, J. J. Richardson, Y. Yan, K. Peter, D. Von Elverfeldt, C. E. Hagemeyer, *Angew. Chem. Int. Ed*. 2014, **53**, 5546-5551.

5 F. Liu, X. He, H. Chen, J. Zhang, H. Zhang, Z. Wang, *Nat. Commun*. 2015, **6**, 8003.

6 G. Zhao, H. Wu, R. Feng, D. Wang, P. Xu, P. Jiang, K. Yang, H. Wang, Z. Guo, Q. Chen, *ACS Appl. Mater. Interfaces* 2018, **10**, 3295-3304.

7 L. Chen, J. Chen, S. Qiu, L. Wen, Y. Wu, Y. Hou, Y. Wang, J. Zeng, Y. Feng, Z. Li, H. Shan, M. Gao, *Small* 2018, **14**, 1702700.

8 Q. Jin, W. Zhu, D. Jiang, R. Zhang, C. J. Kutyreff, J. W. Engle, P. Huang, W. Cai, Z. Liu, L. Cheng, *Nanoscale* 2017, **9**, 12609.